Geophys. J. Int. (2010) **181,** 391–398 doi: 10.1111/j.1365-246X.2009.04494.x

Approximating the wave moduli of double porosity media at low frequencies by a single Zener or Kelvin-Voigt element

Xu Liu,[1,2] Stewart Greenhalgh[2,3] and Bing Zhou[2]

[1] *Centre for Reservoir Geophysics, Imperial College London, South Kensington Campus, London* SW7 2AZ, *UK. E-mail: xu.liu@imperial.ac.uk*
[2] *Department of Physics, University of Adelaide, North Terrace Campus, ADELAIDE* SA 5005, *Australia*
[3] *Institute of Geophysics, ETH Zürich, Zürich* 8092 CH, *Switzerland*

Accepted 2009 December 21. Received 2009 December 21; in original form 2009 August 5

SUMMARY

The analytic transient acoustic wave solution and dispersion characteristics for the double-porosity model are obtained over the whole frequency range for a homogeneous medium. The solution is also obtained by means of approximating the double porosity model with a uniform poro-viscoacoustic model based on a single Zener and a single Kelvin-Voigt (KV) element, respectively. We choose the relaxation function of both mechanical elements which just approximates the dispersion behaviour of the double porosity model around source centre frequencies of 5, 50, 200 and 1000 Hz, respectively. The comparison between the results of the three models shows that if the frequency is much lower than the peak attenuation frequency (4470 Hz) of the example double porosity model, then wave propagation can be well described by the poro-viscoacoustic model with a single Zener element. However, if the frequency is less than 50 Hz, then a single KV element gives an even better result. Therefore, this paper investigates the validity and range of applicability of different single mechanical elements in solving for transient acoustic wave modelling in heterogeneous, double porosity media. The primary attraction of using a Zener model or a KV model is that it allows the convolution integral to be replaced by memory equations by which the field quantities calculated at every time step need not be stored.

Key words: Numerical approximations and analysis; Permeability and porosity; Elasticity and anelasticity; Seismic attenuation.

1 INTRODUCTION

It is well known that the global flow mechanism of Biot theory (Biot 1956, 1962) of porous-media acoustics ignores all wave-induced flow at mesoscopic scales, that is, scales greater than the grain size but less that the wavelength. Biot's theory when applied to homogeneous media cannot explain the high level of attenuation observed in natural porous media such as fluid-filled sands or sandstone over the seismic frequency range (10–200 Hz). This attenuation is successfully described by the mesoscopic heterogeneity models (e.g. White 1975; Dutta & Odé 1979a,b; Gurevich & Lopatnikov 1995; Gelinksy & Shapiro 1997; Johnson 2001; Carcione 2007). By applying the volume averaging theory to the local Biot poroelastic law, Pride & Berryman (2003a,b) developed the double-porosity, dual permeability (DPDP) model. It provides a theoretical framework, including the field equations governing the linear acoustics of composites with two isotropic porous constituents (phase 1 and phase 2), to model acoustic wave propagation through heterogeneous porous structures. Under the assumption that phase 2 is entirely embedded in phase 1, the double-porosity theory is reduced to the effective Biot theory involving complex frequency-dependent elastic moduli through which the internal mesoscopic flow is incorporated. This theory provides good agreement with actual measurements of attenuation over the seismic and ultrasonic frequency bands (Pride *et al.* 2004). It is very difficult to analytically solve the field equations in heterogeneous double porosity media and no such solutions have been derived. Here, the word 'heterogeneous' means at the macroscopic level, for which the size of the heterogeneity is much larger than a wavelength. This situation requires a numerical approach. As is well known, the presence of the Biot slow *P* wave makes Biot's differential equation stiff at low frequencies. To circumvent this difficulty, Carcione & Quiroga-Goode (1995, 1996) partitioned the governing equation into two sets of differential equations, one stiff and the other non-stiff. The splitting technique is to solve the stiff part analytically and then the non-stiff part by the fourth-order Runge-Kutta algorithm. On the other hand, the energy dissipation mechanisms in the governing equations are represented by convolution integrals which require that all calculation results at every time step have to be stored, thus requiring a very large amount of storage and computer time in transient wave numerical modelling. To circumvent this difficulty, Carcione (1996, 1998) successfully applied the standard linear solid (or Zener) model to replace Biot's

© 2010 The Authors
Journal compilation © 2010 RAS

viscodynamic operators in the high frequency range (Biot mechanism) and the squirt flow energy dissipation mechanism (Dvorkin *et al*. 1994). This allows the convolution integral to be replaced by memory equations. If the inner flow energy dissipation mechanism of the DPDP model (Pride *et al.* 2004) can be approximated by a poro-viscoelastic model, then the waves in heterogeneous DPDP medium can be numerically solved based on a poro-viscoelastic method. Liu *et al.* (2009) applied a single Zener mechanical element to replace the attenuation effects in the constitutive equations of the DPDP model and showed that if the frequency is much lower than the peak attenuation frequency of the double porosity model, then wave propagation can be well described by the poro-viscoaoustic model with a single Zener element.

The fact that the frequency dependence of the KV dissipation factor is directly proportional to the frequency is consistent with the attenuation characteristics of the mesoscopic inhomogeneity model or the patchy saturation model at very low frequency, that is, at the tail of the mesoscopic attenuation peak. Therefore, it is possible that the Kelvin-Voigt (KV) element instead of the Zener element might better approximate DPDP model. If so, the KV element will provide a better result in numerical modelling at low frequencies. Furthermore, in numerical modelling, the stress–strain relation based on the KV element has the advantage of not requiring additional field variables (Carcione *et al.* 2004). However, this predication needs to be verified. In this paper, we investigate the validity of the KV model, and compare it with the Zener model to determine the range of applicability and preference between the two models.

2 THE ANALYTICAL SOLUTION FOR A HOMOGENEOUS MEDIUM

2.1 Double porosity model

The double porosity model (or effective single-porosity Biot theory developed by Pride *et al.* 2003a,b, 2004) includes the constitutive equations, the linear transport law and the linear momentum conservation law. Under a time dependence of $e^{-i\omega t}$, the frequency-domain constitutive equations can be written as

$$\frac{1}{i\omega}\begin{bmatrix}\nabla\cdot\mathbf{v}\\ \nabla\cdot\mathbf{q}\end{bmatrix}=\begin{bmatrix}a_{11}^* & a_{12}^*\\ a_{12}^* & a_{22}^*\end{bmatrix}\begin{bmatrix}p_c\\ p_f\end{bmatrix}. \tag{1}$$

Here $\mathbf{v}$ is the average particle velocity of the solid grains; $\mathbf{q}$ is the macroscopic fluid flux through phase 1; p_c is the average total pressure; p_f is the average fluid pressure within the host phase1. The coefficients a_{mn}^* $(m,n=1,2)$ depend on material parameters and frequency ω. They are given in full in Appendix A of our companion paper (Liu *et al.* 2009). The physical meaning of the coefficients can be easily illustrated through their relationship with the familiar effective Biot–Gassmann parameters:

$$\begin{bmatrix}a_{11}^* & a_{12}^*\\ a_{12}^* & a_{22}^*\end{bmatrix}=\frac{1}{K_d(\omega)}\begin{bmatrix}1 & -\alpha(\omega)\\ -\alpha(\omega) & \alpha(\omega)/B(\omega)\end{bmatrix}. \tag{2}$$

Here the frequency dependent parameters $K_d(\omega)$, $K(\omega)$, $\alpha(\omega)$ and $B(\omega)$ refer to the drained bulk modulus, the undrained bulk modulus, the Biot–Willis coefficient and the Skempton coefficient of the composite, respectively (Pride *et al.* 2003a,b, 2004; Liu *et al.* 2009).

The linear transport law can be stated as

$$\nabla p_f=i\omega\rho_f\mathbf{v}-\frac{\eta}{\kappa^*(\omega)}\mathbf{q}, \tag{3}$$

where ρ_f and η are the density and the viscosity of the pore fluid, respectively; and $\kappa^*(\omega)$ is the dynamic permeability of the composite medium. Pride *et al.* (2003a, 2004) suggested taking the harmonic mean of the constituents as the best way to approximate it

$$\frac{1}{\kappa^*(\omega)}=\frac{1-\nu_2}{\kappa_1(\omega)}+\frac{\nu_2}{\kappa_2(\omega)}. \tag{4}$$

Here, the value of ν_2 is the volume fraction of phase 2; $\kappa_1(\omega)$ and $\kappa_2(\omega)$ are the dynamic permeabilities (Johnson *et al.* 1987) of phase 1 and phase 2. The Johnson formula is very complex and related to several independent constants, specifically the tortuosity T, the hydraulic permeability κ_0, the volume-to-surface ratio Λ and the porosity β

$$\kappa(\omega)=\kappa_0\left[\sqrt{1-i\frac{4\omega}{n_J\omega_r}}-i\frac{\omega}{\omega_r}\right], \tag{5}$$

where $\omega_r=\eta\beta/\rho_f T\kappa_0$ and $n_J=\Lambda^2\beta/\kappa_0 T$. We set $n_J=8$ (suggested by Pride *et al.* (2004))and $T=\beta^{-2/3}$ for simplicity.

It is important to point out that the harmonic mean of the constituents eq. (4) can be replaced by the formula given by Miloh & Benveniste (1988). Although not given in this paper, it is not difficult to prove that if ν_2 is small, the Miloh and Benveniste formula gives a very similar result to the harmonic mean for very high permeability of phase 2 and the arithmetic mean for very low permeability of phase 2.

The conservation of linear momentum equation is expressed as

$$\nabla p_c=i\omega\left(\rho\mathbf{v}+\rho_f\mathbf{q}\right), \tag{6}$$

where ρ is the total average density of the composite.

Eqs (1), (3) and (6) are the governing equations in the frequency-domain for the double porosity model with a fully embedded phase 2.

The acoustic wave dispersion characteristics can be easily obtained. Taking the divergence of eqs (3) and (6), combining with eq. (1), eliminating the $\mathbf{v}$ and $\mathbf{q}$ terms, and adding in a source force term S, we obtain

$$\Delta\left(\mathbf{P}-\mathbf{S}\right)+\omega^2\mathbf{D}\cdot\mathbf{P}=0, \tag{7}$$

where

$$\mathbf{P}=\begin{bmatrix}p_c\\ p_f\end{bmatrix},\quad \mathbf{S}=\begin{bmatrix}S\\ S_f\end{bmatrix}\quad\text{and}\quad \mathbf{D}=\mathbf{\Gamma}\cdot\mathbf{M} \tag{8}$$

with

$$\mathbf{\Gamma}=\begin{bmatrix}\rho & \rho_f\\ \rho_f & -\dfrac{\eta}{i\omega\kappa^*(\omega)}\end{bmatrix},\quad \mathbf{M}=\begin{bmatrix}a_{11}^* & a_{12}^*\\ a_{12}^* & a_{22}^*\end{bmatrix}. \tag{9}$$

Comparing eq. (7) with eq. (26) in the paper by Carcione & Quiroga-Goode (1996), we find that there are some differences. On the one hand, the a_{ij}^* elements of the $\mathbf{M}$ matrix are complex frequency-dependent values (see Liu *et al.* 2009), while the corresponding elements in Carcione's eq. (26) are real values. On the other hand, the effective permeability $\kappa^*(\omega)$ in the $\mathbf{\Gamma}$ matrix of eq. (9) is defined by eq. (4) and it's frequency response depends on the combined response of both porous phases following the Johnson model (Johnson *et al.* 1987). Equation of (4) is assumed to hold true over the full frequency range (low and high frequencies), while Carcione & Quiroga-Goode (1996) use the simplification for $\frac{\eta}{\kappa^*(\omega)}$ given by Biot (1962) at low frequency and that given by Auriault *et al.* (1985)

at high frequency, respectively. Following their approach, eq. (7) can be solved to get the characteristic equation

$$\det\left[\mathbf{D}-\left(\frac{k}{\omega}\right)^2\mathbf{I}\right]=0, \tag{10}$$

where $k=|\mathbf{k}|$, and $\mathbf{k}$ is the complex wavevector. If the eigenvalues of $\mathbf{D}$ are $\lambda_{1(2)}$, then the complex velocities are given by

$$V_v=\frac{1}{\sqrt{\lambda_v}},\qquad v=1,2, \tag{11}$$

where $v=1,2$ corresponds to the fast and the slow P waves, respectively.

The phase velocities c_v and quality factors Q_v can be expressed as

$$c_v(\omega)=\left[\mathrm{Re}\left(\frac{1}{V_v}\right)\right]^{-1}\quad\text{and}\quad Q_v(\omega)=\frac{\mathrm{Re}\left[V_v^2\right]}{\mathrm{Im}\left[V_v^2\right]}. \tag{12}$$

The Biot slow P wave is very difficult to measure because of the extremely high attenuation. In this paper, we focus on the fast or classical P wave.

Following Carcione & Quiroga-Goode (1996) and Carcione (2007), the transient solution of eq. (7) is shown to be

$$\mathbf{P}=G(\mathbf{D})\cdot\mathbf{S}h(\omega), \tag{13}$$

where

$$G(\mathbf{D})=\frac{1}{\lambda_1-\lambda_2}\left\{\left[G(\lambda_1)-G(\lambda_2)\right]\mathbf{D}+\left[\lambda_1G(\lambda_2)-\lambda_2G(\lambda_1)\right]\mathbf{I}\right\}, \tag{14}$$

$$G(\lambda_v)=-\left[\omega^2\lambda_v g(\lambda_v)+8\delta(\mathbf{x})\right]\,v=1,2, \tag{15}$$

$$\begin{cases} g(\lambda_v)=-2iH_0^{(2)}\left[\omega r\sqrt{\lambda_v(\omega)}\right] \\ r=\sqrt{x^2+z^2} \end{cases}\text{for the 2-D solution (linesource)}, \tag{16}$$

$$\begin{cases} g(\lambda_v)=\dfrac{1}{r}\exp\left[-\mathrm{i}\omega r\sqrt{\lambda_v(\omega)}\right] \\ r=\sqrt{x^2+y^2+z^2} \end{cases}\text{for the 3-D solution (point source)}. \tag{17}$$

Here $H_0^{(2)}$ is the Hankel function of the second kind, $\mathbf{S}=[\mathrm{S},\mathrm{S_f}]$ is a constant vector and set as $\mathbf{S}=[1,1]$ in this paper, while $h(\omega)$ represents the source frequency spectrum.

The analytical solution in the time domain can be obtained by an inverse Fourier transformation.

For the following example, we choose the source to be a Ricker wavelet time function given by Carcione & Quiroga-Goode (1995) as

$$f(t)=\exp\left[-\frac{1}{2}f_c^2(t-t_0)^2\right]\cos\left[\pi f_c(t-t_0)\right], \tag{18}$$

where $t_0=3/.f_c$ and f_c is the centre frequency.

To compare with the numerical solutions in the following sections, the source term in eq. (13) should be written as

$$h(\omega)=\frac{F[f(t)]}{\mathrm{i}\omega}, \tag{19}$$

where $F(f(t))$ means the Fourier transform of $f(t)$.

2.2 Poro-viscoacoustic model

Based on the double porosity model, the poro-viscoacoustic model is obtained by replacing the complex modulus in the constitutive equations by the viscoacoustic model (Carcione 2007).

Eq. (1) can be rewritten as

$$\mathrm{i}\omega\begin{bmatrix}p_c(\omega)\\ p_f(\omega)\end{bmatrix}=\begin{bmatrix}a_{11}^{-*}(\omega) & a_{12}^{-*}(\omega)\\ a_{12}^{-*}(\omega) & a_{22}^{-*}(\omega)\end{bmatrix}\begin{bmatrix}\nabla\cdot\mathbf{v}(\omega)\\ \nabla\cdot\mathbf{q}(\omega)\end{bmatrix}, \tag{20}$$

where $a_{ij}^{-*}(\omega)$ is the complex element of the inverse matrix of $\mathbf{M}$.

We use the Zener model or KV model to represent the relaxation functions and investigate the discrepancy between the replacement and the double porosity model.

The complex modulus of a Zener element is given by Carcione (1996, 2007) as

$$M_Z(\omega)=M_Z^R\frac{1-\mathrm{i}\omega\tau^\varepsilon}{1-\mathrm{i}\omega\tau^\sigma}. \tag{21}$$

Here M_Z^R, τ^ε and τ^σ are the relaxed modulus, the strain relaxation time and the stress relaxation time of the Zener element, respectively.

The complex modulus of a KV element is given by Carcione (2007) as

$$M_K(\omega)=M_K^R\left(1+\mathrm{i}\omega\tau\right). \tag{22}$$

Here M_K^R and τ are the relaxed modulus and the relaxation time of the KV element, respectively.

Setting the relaxed modulus of each element of the complex modulus matrix in eq. (20) to be equal to that of the Zener or the KV element ($M_{K,Z}^R=a_{ij}^{-*}(\omega=0)$), and the same relaxation time for each matrix element (because of the assumption of a single Zener or KV element) leads to

$$i\omega\begin{bmatrix}p_c(\omega)\\ p_f(\omega)\end{bmatrix}=M_X\begin{bmatrix}a_{11}^{-*}(\omega=0) & a_{12}^{-*}(\omega=0)\\ a_{12}^{-*}(\omega=0) & a_{22}^{-*}(\omega=0)\end{bmatrix}\begin{bmatrix}\nabla\cdot\mathbf{v}(\omega)\\ \nabla\cdot\mathbf{q}(\omega)\end{bmatrix}. \tag{23}$$

Here,

$$\left.\begin{array}{ll} M_X=\dfrac{1-i\omega\tau^\varepsilon}{1-i\omega\tau^\sigma} & \text{for the Zener model}\\ M_X=1+i\omega\tau & \text{for the KV model}\end{array}\right\}. \tag{24}$$

In the double porosity model, except for the Biot dissipation mechanism which acts at very high frequency, the local mesoscopic flow (or inner flow) is the dominant dissipation mechanism in the seismic frequency band; its behaviour is incorporated into the complex modulus (see eqs 2 and 23). This inner flow model represents the dissipation mechanism for both the solid frame and the pore fluid and thus can be approximated by the same Zener or the same KV model for the four complex moduli in eq. (23). This is the reason why M_X is the common factor for the modulus matrix (see eq. (23)). Otherwise four different Zener or KV elements for each element of the complex modulus matrix in eq. (20) have to be used. Furthermore, we assume a single Zener element with one set of relaxation times which means τ^ε and τ^σ. For a single KV element, just one relaxation time τ needs to be determined.

Eqs (23), (6) and (3) are the governing equations of the poro-viscoacoustic model in the frequency domain.

© 2010 The Authors, *GJI*, **181,** 391–398
Journal compilation © 2010 RAS

Table 1. Material properties of the sample rocks and fluids

Grain and fluid Parameter	Grains	Parameter	Water
K_s (N m^{-2})	3.9E+10	K_f (N m^{-2})	2.25×10^9
G_s (N m^{-2})	4.4E+10	ρ_f (kg m^{-3})	1000
ρ_s (kg m^{-3})	2650.0	η_f (kg m^{-1}s^{-1})	0.001

Materials B (corresponding to 10 m depth double porosity sandstone)

Parameter	Phase 1	Phase 2	Parameter	Composite
K_{dj} (N m^{-2})	2.23E10	2.04E8	K_d (N m^{-2})	7.85E9
G_{dj} (N m^{-2})	2.20E10	1.22E8	G_d (N m^{-2})	5.98E9
L1 (m)	0.0086	0.0086	ν_2	0.03
β_j	0.20	0.36	β	$\beta=(1-\nu_2)\beta_1+\nu_2\beta_2$
κ_{0j}(m^2)	1.0E-14	1.0E-9	κ_0(m^2)	$1/\kappa_0=(1-\nu_2)/\kappa_{01}+\nu_2/\kappa_{02}$
Λ(m)	0.005	$T=\beta^{-2/3}$		

Notes: The physical meaning of the various parameters (Pride *et al.* 2004).
Subscript j denoting Phase 1 or 2; $K_{s,d,f}$ is bulk modulus of grain(s), drained porous frame (d) or fluid (f), respectively; $G_{s,d}$ shear modulus of grain and porous frame; $\rho_{s,f}$ density of grain or fluid; η_f viscosity; L1 is the characteristic length of the fluid pressure gradient; $\nu_2$volume fraction of phase 2; β porosity; κ_0 hydraulic permeability; Λ volume-to-surface ratio; T is tortuosity.

Taking the divergence of Eqs (6), (3) combining with eq. (23) and eliminating $\mathbf{v}(\omega)$ and $\mathbf{q}(\omega)$, we obtain the dispersion equation for homogeneous poro-viscoacoustic waves. It can be expressed by

$$\Delta\begin{bmatrix}p_c\\ p_f\end{bmatrix}+\frac{\omega^2}{M_X}\begin{bmatrix}\rho & \rho_f\\ \rho_f & -\dfrac{\eta}{i\omega\kappa^*(\omega)}\end{bmatrix}\times\begin{bmatrix}a_{11}^*(\omega=0) & a_{12}^*(\omega=0)\\ a_{21}^*(\omega=0) & a_{22}^*(\omega=0)\end{bmatrix}\begin{bmatrix}p_c\\ p_f\end{bmatrix}=0. \quad (25)$$

Adding in a source force term $\mathbf{S}$ to the above equation and rewriting it we get

$$\Delta(\mathbf{P}-\mathbf{S})+\omega^2\Gamma\cdot N\cdot P=0, \quad (26)$$

where $\mathbf{S}$ and $\mathbf{\Gamma}$ are defined in eqs (8) and (9). The other terms are defined by

$$\mathbf{P}=\begin{bmatrix}p_c\\ p_f\end{bmatrix}\quad\text{and}\quad\mathbf{N}=\begin{bmatrix}a_{11}^*(\omega=0) & a_{12}^*(\omega=0)\\ a_{21}^*(\omega=0) & a_{22}^*(\omega=0)\end{bmatrix}\Big/M_X. \quad (27)$$

The eigenvalues $\mathbf{\Gamma}\cdot\mathbf{N}$ are denoted as $\hat{\lambda}_{1,2}$.

Similarly, the transient solution of (26) can be obtained by replacing λ_1 and λ_2 in (16) and (17) with $\hat{\lambda}_1$ and $\hat{\lambda}_2$, respectively. The hat symbol '^' above λ implies the value of the poro-viscoacoustic model.

Now we use the dispersion curves of the double porosity model to determine the relaxation times of the poro-viscoacoustic model by the following method.

For the Zener model

$$\tau^{\varepsilon}=\frac{1}{2\pi f_c}\left[\sqrt{Q^2(f_c)+1}+1\right]\quad\text{and}$$
$$\tau^{\sigma}=\frac{1}{2\pi f_c}\left[\sqrt{Q^2(f_c)+1}-1\right] \quad (28)$$

For the KV model

$$\tau=\frac{1}{2\pi f_c Q(f_c)}. \quad (29)$$

To fully represent the double porosity model means that the KV or Zener elements should be chosen to make $\hat{\lambda}_{1,2}=\lambda_{1,2}$ over the whole frequency range. It should be noted that the phase velocity of the double porosity model $c(f_c)$ does not enter into the eigenvalues of the wave equation (26), which actually depends on $c(f=0)$(see eq. 27). Therefore, we need to compare the dispersion characteristics between DPDP model and the poro-viscoacoustic model.

3 COMPARSION

We now wish to compare the range of applicability and the consistency between the two poro-viscoacoustic models and the DPDP model. We do so by means of specific examples. We use a sample double porosity material having sandstone as the host rock (phase 1) and a volume fraction 3% of sand as the inclusions (phase 2). The material corresponds to a burial depth of 10 m according to Walton theory and the Hashin and Shtrikman bound (see Pride *et al.* 2004, for details).This material was denoted as material B in the companion paper (Liu *et al.* 2009). Its properties are listed here in Table 1.

The phase velocity $c(f_p)$ and attenuation $1/Q(f_p)$dispersion curves of the double porosity model are computed and shown as the solid lines in fig. 2 of Liu *et al.* (2009). The behaviour over the low frequency range will be shown later in the present paper. The peak value of $1/.Q(f_p)$ is 0.0972 ($Q\cong10$) and f_p is 4471 Hz, with a corresponding phase velocity of $c(f_p)$ of 2757 m s^{-1}. The peak frequency f_p refers to the frequency at which the mesoscopic structure just has time to equilibrate in one cycle.

The wave pulse used in field seismic exploration is usually at much lower frequencies, less than several hundred Hz, and has a relatively narrow band. This means that for frequency dependent-material properties, only the values around the centre frequency of the seismic source f_c will determine the wave propagation. Therefore, we choose the relaxation function which just needs to approximate the dispersion behaviour of the double porosity model around f_c, which is also the peak frequency of the Zener element. Since the dissipation factor of a KV element is directly proportional to frequency, there is no peak value. This method makes sure that there is good agreement between the attenuation of the two poro-viscoacoustic models and that of the double porosity model at the centre frequency f_c, but the agreement of the phase velocity depends on f_c. We choose four different frequencies, f_c equal to 5, 50 200 and 1000 Hz. The dispersion values of $\hat{c}(f_c)$ and $1/.\hat{Q}(f_c)$ of the three different models at the peak frequency are shown in Table 2. Our method makes sure that both the KV element and the Zener

Table 2. Phase velocity c and specific quality factor Q dispersion values at the peak (DPDP model) or central frequency (Zener or Kelvin Voigt models)

Frequency	Quality factor	Velocity ($\mathrm{m\,s^{-1}}$) DPDP	Velocity ($\mathrm{m\,s^{-1}}$) Zener	Velocity ($\mathrm{s^{-1}}$) KV
f_p4470 Hz	$Q(f_p)$10	2757	2583 (6.3 per cent)	
f_c1000 Hz	$Q(f_c)$12	2628	2566 (2.4 per cent)	2464 (6.2 per cent)
f_c200 Hz	$Q(f_c)$17	2530	2533 (0.1 per cent)	2460 (2.7 per cent)
f_c50 Hz	$Q(f_c)$30	2474	2498 (1.0 per cent)	2458 (0.6 per cent)
f_c5 Hz	$Q(f_c)$248	2458	2462 (0.2 per cent)	2457 (0.04 per cent)

Note: Values in brackets mean the relative difference: $|\hat{c}(f_c) - c(f_c)|/\max[\hat{c}(f_c),\ c(f_c)]$.

element have the same values of $1/\hat{Q}(f_c)$ as that of DPDP model at the centre frequency, therefore only the phase velocity values $\hat{c}(f_c)$ values at this frequency are listed in Table 2. We also use the relative differences of the phase velocity values at the central frequencies (Table 2) to estimate the deviation of the dispersion curves between DPDP model and Zener or KV model. It is clear that the KV element gives excellent agreement (the relative difference is less than 0.04 per cent) with the peak velocity of the DPDP model at f_c of 5 Hz. The advantage of the KV model is preserved out to a frequency of 50 Hz at which the KV model yields a relative difference of 0.6 per cent compared to 1.0 per cent for the Zener model. However with f_c increasing up to 1000 Hz, the relative difference for the KV model rises to 6 per cent. By comparison, at f_c of 5 and 50 Hz the Zener element has relative differences to the DPDP model of 0.16 and 1.0 per cent, respectively which is not as good as that of the KV element. However with f_c increasing up to 1000 Hz, the relative difference is less than 2.3 per cent which is much better than those of KV element.

The comparison of the three models is also shown in both dispersion curves of $\hat{c}(f_c)$ and $1/\hat{Q}(f_c)$. In addition, we have computed the transient waveform solutions for the DPDP, Zener and KV models using Ricker-type source wavelets having centre frequencies of 5, 50, 200 and 1000 Hz. In the following figures, the solid lines (denoted with D) are the results for the double porosity model (see fig. 2 of Liu *et al.* (2009) for its dispersion over the whole frequency range) having the peak attenuation frequency of the double porosity model of 4471 Hz. The dashed lines (denoted with Z) are for a porous-viscoacoustic material with a single Zener relaxation function. The dotted lines (denoted with K) are for a porous-viscoacoustic material with a KV relaxation function. The difference between the solid line and the dashed line or dotted lines shows the effect of the approximation by single Zener or KV elements. At the centre frequencies, the dissipation factors of the porous-viscoacoustic models are set to be equal to that of DPDP model.

Fig. 1 shows the dispersion curves for $f_c = 5$ Hz on the left-hand side and for $f_c = 50$ Hz on the right-hand side. Noting the small scales on the vertical axes, the *P*-wave phase velocity (upper diagram) and dissipation factor (lower diagram) dispersion curves for f_c values of 5 and 50 Hz show very good consistency between the two poro-viscoacoustic (KV, Zener) models and the DPDP model. In particular, the dispersion characteristics of the KV model around 5 Hz are in excellent agreement with those of the DPDP model.

We have calculated 2-D analytical transient solutions of the average pressure wave p_c and the average fluid pressure wave p_f in the example homogeneous double porosity material with the three models. For every centre frequency, the waveforms at two distances (near the source and far from the source) were computed. The amplitudes of p_c and p_f were normalized to the peak value of p_c at a distance near the source.

Figs 2 and 3 show the computed waveforms for a source centre frequency f_c of 5 Hz and receiver distances of 2828 and 8485 m, and a f_c of 50 Hz and receiver distances of 283 and 849 m, respectively. Both figures show a good match between the two mechanical elements and the DPDP model.

Fig. 4 shows the dispersion curves for $f_c = 200$ Hz (the left-hand side) and $f_c = 1000$ Hz (the right-hand side). The *P*-wave phase velocity (upper diagrams) and the dissipation factor (lower diagrams) dispersion curves for an f_c of 200 Hz show a very good consistency between the Zener model and the DPDP model. However, the phase velocity for the KV model exhibits a significant discrepancy from that for the DPDP model. For $f_c = 1000$ Hz the dispersion patterns for both the Zener element and the KV element deviate from those of the DPDP model.

Figs 5 and 6 show the computed waveforms for a f_c of 200 Hz and receiver distances of 71 and 212 m, and a f_c of 1000 Hz and receiver distances of 14.1 and 42.3 m, respectively. It is clear from Fig. 5 that the Zener model has a much better agreement with the DPDP result than does the KV model for waves having frequencies of around 200 Hz. Fig. 6 for $f_c = 1000$ Hz shows a poor match between the two mechanical elements and the DPDP model. Therefore, neither such single viscoacoustic element can be applied to approximate the wave behaviour in a DPDP medium at high frequencies.

The above comparisons provide a means for checking the validity of the approximations. If an acoustic wave in a heterogeneous double porosity medium needs to be numerically simulated through the approximation of the poro-viscoacoustic model, then the source centre frequency should be much lower than the lowest peak attenuation frequency of every component making up the heterogeneous medium. A numerical method for modelling acoustic waves in DPDP media based on the approximation by the Zener element has been reported by Carcione (1996, 1998, 2007), Carcione & Seriani (2001) and Liu *et al.* (2009). The corresponding extension to the KV element is given by Carcione *et al.* (2004).

4 CONCLUSIONS

We have analytically solved for the phase velocity and dissipation factor (attenuation) dispersion characteristics, as well as the analytic transient pressure waveform for a homogeneous acoustic double porosity model and for a poro-viscoacoustic model based on the Zener and the KV elements, respectively. By the method of fitting the relaxation times to the value of the quality factor of the double porosity model at the centre frequency of the source, we find that the KV model is a reasonable option to replace the Zener element at very low frequency, for example, less than 50 Hz. For our sample rock at f_c of 5 and 50 Hz the relative differences of the phase velocity with the DPDP model are less than 0.04 and 0.6 per cent for the KV element compared to 0.16 and 1.0 per cent

© 2010 The Authors, *GJI*, **181,** 391–398
Journal compilation © 2010 RAS

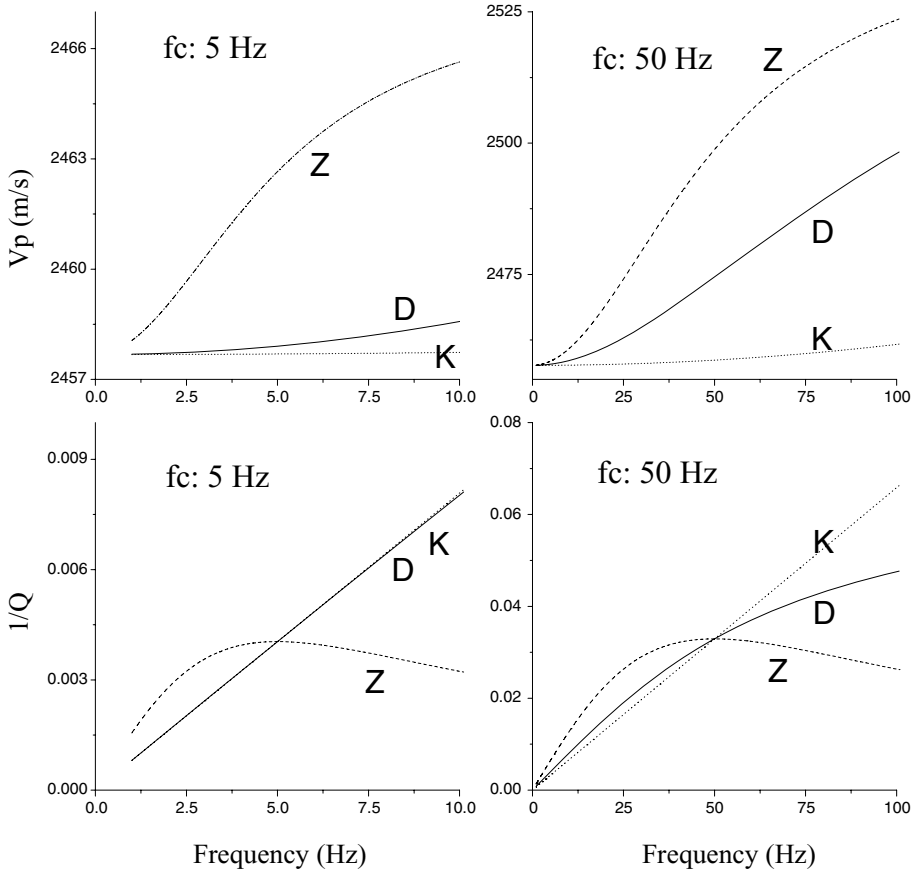

Figure 1. The dispersion curves of phase velocity (upper) and specific dissipation factor (lower) for the sample material. The two porous-viscoacoustic material have relaxation frequency of 5 and 50 Hz on the left-hand side and on the right-hand side, respectively. KV model around 5 Hz are in excellent agreement with those of the DPDP model.

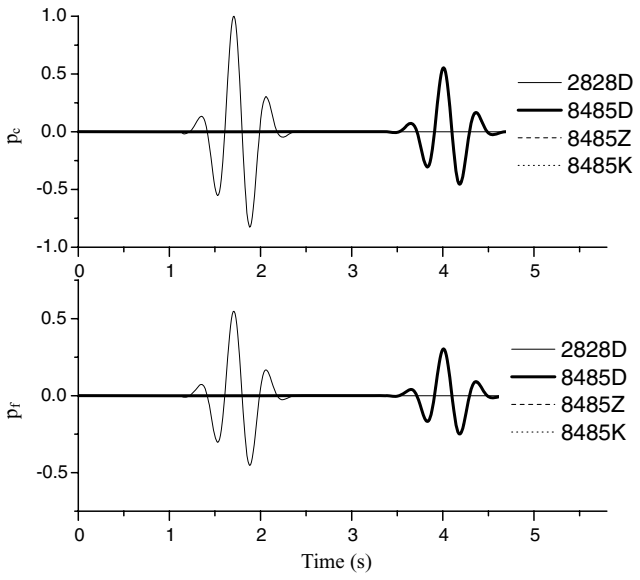

Figure 2. Analytical solution for pressure p_c (upper) and p_f (lower). The source pulse has a centre frequency of 5 Hz. The numbers 2828 and 8485 denote the source–receiver distances of 2828 m and 8485 m. At the same distance, the curves for both Zener and KV models show a very good match with the DPDP model.

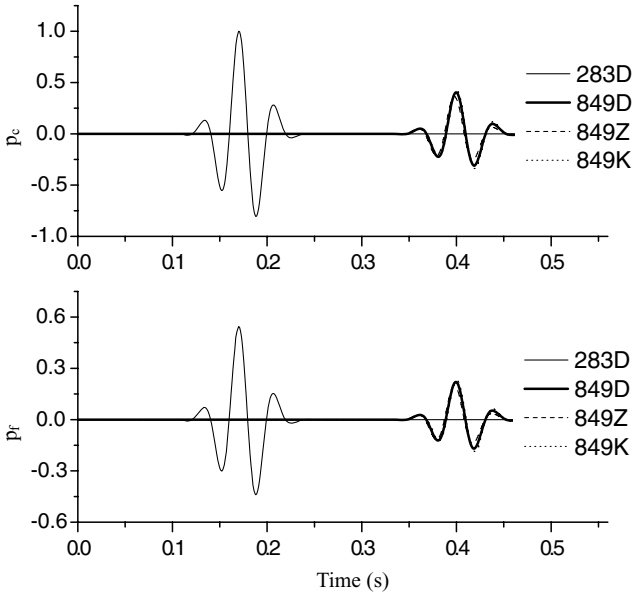

Figure 3. Analytical solution for pressure p_c (upper) and p_f (lower). The source pulse has a centre frequency of 50 Hz. The numbers 283 and 849 denote the source–receiver distances of 283 and 849 m. At the same distance, the curves (dashed and solid lines) for both the Zener and the KV model show a very good match.

© 2010 The Authors, *GJI*, **181,** 391–398
Journal compilation © 2010 RAS

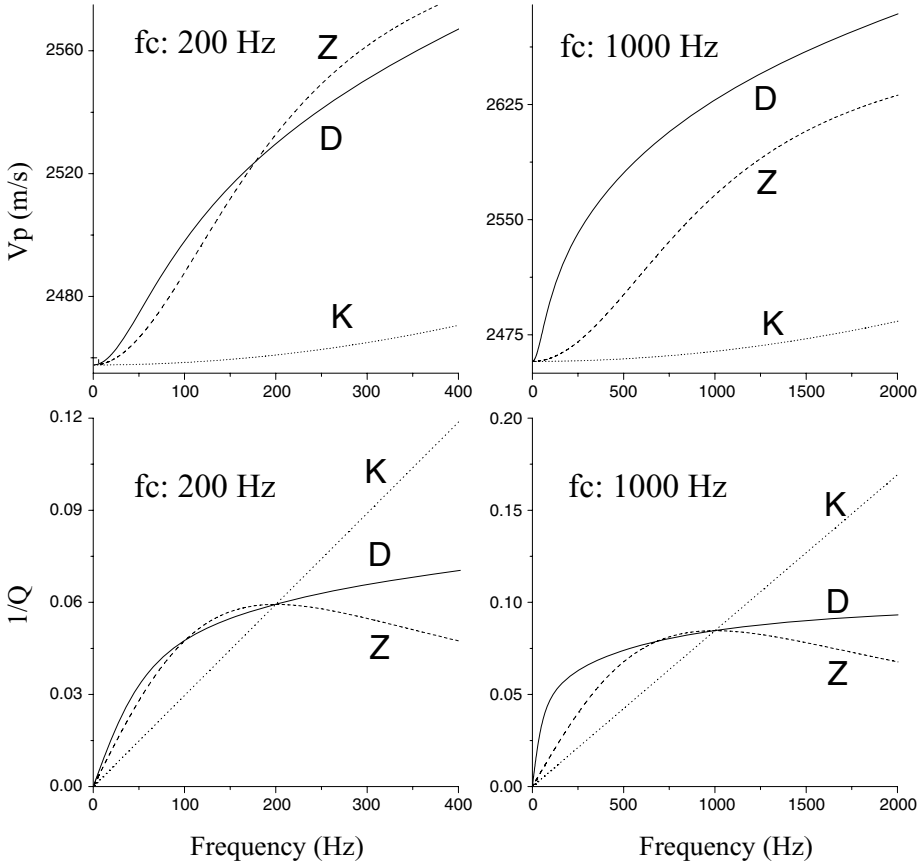

Figure 4. The dispersion curves of phase velocity (upper) and specific dissipation factor (lower) for the sample material. The two porous-viscoacoustic material have relaxation frequency of 200 and 1000 Hz on the left-hand side and on the right-hand side, respectively.

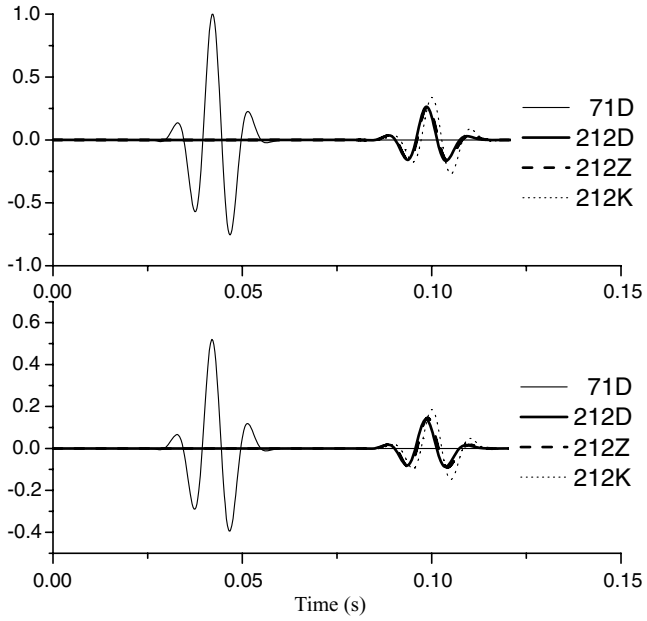

Figure 5. Analytical solution for pressure p_c (upper) and p_f (lower). The source pulse has a centre frequency of 200 Hz. The numbers 71 and 212 denote the source–receiver distances of 71 and 212 m. At the same distance, the curves (dashed and solid lines) show that the DPDP model and the Zener model have a very good match, but the KV model has a significant discrepancy.

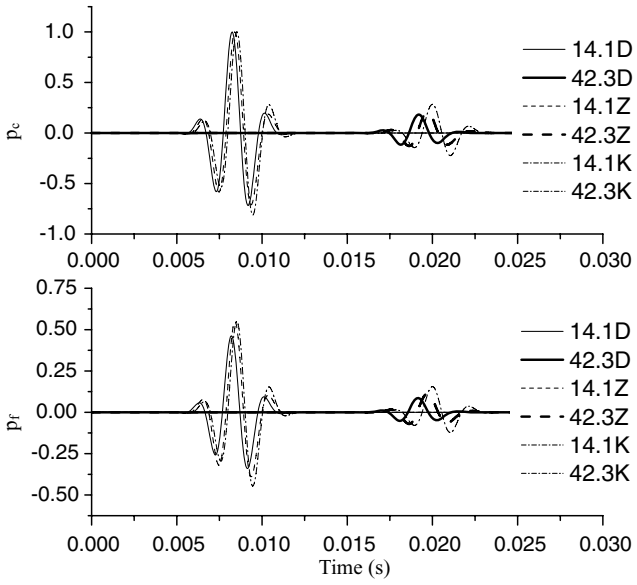

Figure 6. Analytical solution for pressure p_c (upper) and p_f (lower). The source pulse has a centre frequency of 1000 Hz. The numbers 14.1 and 42.3 denote the source–receiver distances of 14.1 and 42.3 m. At the same distance, the curves (dashed and solid lines) for both the Zener and the KV model do not match with the DPDP model.

© 2010 The Authors, *GJI*, **181,** 391–398
Journal compilation © 2010 RAS

for the Zener element. This suggests that the KV model is better than the Zener model in numerical modelling of low frequency earthquake waves. However, when f_c is larger than several hundred hertz, the KV model yields significant discrepancy with the DPDP model. For example, the relative difference changes from 2.8 to 6 per cent for f_c of 200 and 1000 Hz, respectively. By contrast, the Zener element gives better agreement, with a relative difference of just 0.12 per cent at f_c of 200 Hz. If f_c is larger than 1000 Hz, both methods deviate from the DPDP model, with significant discrepancies in the relative differences being larger than 2.3 per cent. The comparisons given in this paper clarify the utility and preference between the two single-mechanical elements to approximate the acoustic wave behaviour in DPDP media. Our conclusion is based on the sample material in this paper. The validity and preference offered by the method depend on the actual porous material used in the numerical modelling and on the size of rock model. It is important to check the validity for every material component before numerical modelling.

This paper investigates the validity and range of applicability of a Zener model or a KV model in transient acoustic wave modelling in heterogeneous double porosity media. The importance and significance of applying the two poro-viscoacoustic models is that they allow the convolution integral to be replaced by memory equations for which the calculated field quantities at every time step need not be stored.

ACKNOWLEDGMENTS

The authors thank Dr J. Carcione for his suggestion which motivated us to pursue the research of this paper. We also wish to thank Dr E Saenger and an anonymous reviewer for their constructive reviews which helped improve the manuscript.

REFERENCES

Auriault, J.L, Borne, L. & Chambon, R., 1985. Dynamics of porous saturated media, checking of the generalized law of Darcy, *J. acoust. Soc. Am.,* **77,** 1641–1650.

Biot, M.A, 1956. Theory of propagation of elastic waves in a fluid-saturated porous solid. I: low-frequency range, *J. acoust. Soc. Am.,* **28**(2), 168–178.

Biot, M.A., 1962. Mechanics of deformation and acoustic propagation in porous media, *J. appl. Phys.,* **33**(4), 1482–1498.

Carcione, J.M., 1996. Wave propagation in anisotropic, saturated porous media: plane-wave theory and numerical simulation, *J. acoust. Soc. Am.,* **99**(5), 2655–2666.

Carcione, J.M., 1998. Viscoelastic effective rheologies for modelling wave propagation in porous media, *Geophys. Prospect.,* **46,** 249–270.

Carcione, J.M., 2007. *Wave Fields in Real Media: Wave Propagation in Anisotropic, Anelastic, Porous and Electromagnetic Media, Handbook of Geophysical Exploration, Seismic Exploration,* Vol. **38**, 2nd edn (Revised and Extended) eds Helbig, K. & Treitel, S. Elsevier Ltd, Oxford, UK-Amsterdam, The Netherlands.

Carcione, J.M. & Quiroga-Goode, G., 1995. Some aspects of the physics and numerical modelling of Biot compressional waves, *J. Comput. Acoust.,* **3**(4), 261–280.

Carcione, J.M. & Quiroga-Goode, G., 1996. Full frequency-range transient solution for compressional waves in a fluid-saturated viscoacoustic porous medium, *Geophys. Prospect.,* **44,** 99–129.

Carcione, J.M. & Seriani, G., 2001. Wave simulation in frozen porous media, *J. Comput. Phys.,* **170**, 676–695.

Carcione, J.M., Poletto, F. & Gei, D., 2004. 3-D wave simulation in anelastic media using the Kelvin-Voigt constitutive equation, *J. Comput. Phys.,* **196,** 282–287.

Dvorkin, J., Nolen-Hoeksema, R. & Nur, A., 1994. The squirt-flow mechanism: macroscopic description, *Geophysics,* **59**(3), 428–438.

Dutta, N.C. & Odé, H., 1979a. Attenuation and dispersion of compressional waves in fluid-filled porous rocks with partial gas saturation (White model). Part I: Biot theory, *Geophysics,* **44**(11), 1777–1788.

Dutta, N.C. & Odé, H., 1979b. Attenuation and dispersion of compressional waves in fluid-filled porous rocks with partial gas saturation (White model). Part II: results, *Geophysics,* **44**(11), 1789–1805.

Gelinksy, S. & Shapiro, S.A., 1997. Dynamic-equivalent medium approach for thinly layered saturated sediments, *Geophys. J. Int.,* **128** (1), F1-F4.

Gurevich, B. & Lopatnikov, S.L., 1995. Velocity and attenuation of elastic waves in finely layered porous rocks, *Geophys. J. Int.,* **121**(3), 933–947.

Johnson, D.L., 2001. Theory of frequency dependent acoustics in patchy-saturated porous media, *J. acoust. Soc. Am.,* **110**(2), 682–694.

Johnson, D.L., Koplik, J. & Dashen, R., 1987. Theory of dynamic permeability and tortuosity in fluid-saturated porous media, *J. Fluid Mech.,* **176,** 397–402.

Liu, X., Greenhalgh, S. & Zhou, B., 2009. Transient solution for poro-viscoacoustic wave propagation in double porosity media, and its limitations, *Geophys. J. Int.,* **178,** 375–393.

Miloh, T., Benveniste, Y., 1988. A generalized self-consistent method for the effective conductivity of composites with ellipsoidal inclusions and cracked bodies, *J. appl. Phys.,* **63**(3), 789–796.

Pride, S.R. & Berryman, J.G., 2003a. Linear dynamics of double-porosity and dual-permeability materials. I. Governing equations and acoustic attenuation, *Phys. Rev., E,* **68,** 036603.

Pride, S.R. & Berryman, J.G., 2003b. Linear dynamics of double-porosity and dual-permeability materials. II. Fluid transport equations, *Phys. Rev., E,* **68,** 036604.

Pride, S.R., Berryman, J.G. & Harris, J.M., 2004. Seismic attenuation due to wave-induced flow, *J. geophys. Res.,* **109,** B01201.

White, J.E., 1975. Computed seismic speeds and attenuation in rocks with partial gas saturation, *Geophysics,* **40**(2), 224–232.